A STUDY OF THE EQUILIBRIUM VACANCY ENSEMBLE IN
ALUMINUM USING 1D- AND 2D-ANGULAR CORRELATION
OF ANNIHILATION RADIATION

M. J. FLUSS
S. BERKO
B. CHAKRABORTY
K. R. HOFFMAN
P. LIPPEL
R. W. SIEGEL

THIS PAPER WAS PREPARED FOR SUBMITTAL TO THE
PROCEEDINGS OF THE 7TH INTERNATIONAL CONFERENCE
ON POSITRON ANNIHILATION, NEW DELHI, INDIA
JANUARY 6-11, 1985

MARCH 12, 1985

A STUDY OF THE EQUILIBRIUM VACANCY ENSEMBLE IN ALUMINUM USING 1D- AND 2D-ANGULAR CORRELATION OF ANNIHILATION RADIATION[*]

M.J. Fluss[abc], S. Berko[b], B. Chakraborty[ad],
K.R. Hoffmann[b], P. Lippel[b], and R.W. Siegel[a]

[a] Materials Science and Technology Division, Argonne National Laboratory, Argonne, IL 60439, USA

[b] Department of Physics, Brandeis University, Waltham, MA 02254, USA

[c] Present address: Lawrence Livermore National Laboratory, Livermore CA 94550, USA
[d] Present address: Reactor Research Centre, Kalpakkam 603 102, Tamil Nadu, INDIA

One- and two-dimensional angular correlation of positron-electron annihilation radiation (1D and 2D-ACAR) data have been obtained between 293 and 903 K for single crystals of aluminum. The peak counting rates vs temperature, which were measured using the 1D-ACAR technique, provide a model independent value for the temperature dependence of the positron trapping probability. Using these results it is possible to strip out the Bloch state contribution from the observed 2D-ACAR surfaces and then compare the resulting defect ACAR surfaces to calculated 2D-ACAR surfaces for positrons annihilating from the Bloch, monovacancy, and divacancy-trapped states. The result of this comparison is that the presence of an increasing equilibrium divacancy population is consistent with the observed temperature dependence of ACAR data at high temperature in Al and that the present results when compared to earlier studies on Al indicate that the ratio of the trapping rates at divacancies and monovacancies is of order two.

1. EXPERIMENT

The present data (1,2) were obtained at Brandeis Univ. using 1D- and 2D-ACAR instruments (3-5). Peak-count rate 1D-ACAR measurements (2.0 mrad FWHM) were performed for the <100>, <110>, and <111> crystal orientations of Al. Data was accumulated in temperature steps of 5 K so that both monovacancy and mono-divacancy trapping model analyses could be performed on the data. The 2D-ACAR data were obtained for a <100> orientation axis along the integration direction p_x and the <110> axes along p_y and p_z. The angular resolution for these experiments was 1.5 mrad at FWHM so as to maximize the counting rates with the 64 discrete detector 2D-ACAR system. The Al samples, and positron source were maintained in a 38 mm diameter vacuum system at 10^{-7}-10^{-8} Torr and positioned between the pole faces of a 15-20 kG magnet with suitable Pb shielding to shadow the positron source. Fig. 1 shows linear and logarithmic perspective representations for the experimental 2D-ACAR surfaces at 293 K (N(293)), (Bloch state) and two spectra at 613 and 903 K (N_t(613) and N_t(903)) from which the Bloch state contribution has been removed. The peak count rate "S" shaped curve is typical of one of the three crystal orientations and the circles on the curve indicate additional temperatures where 2D-ACAR data were obtained. The slope of the high temperature region of the peak-count rate data is somewhat atypical of most metals. In the case of Al this shape
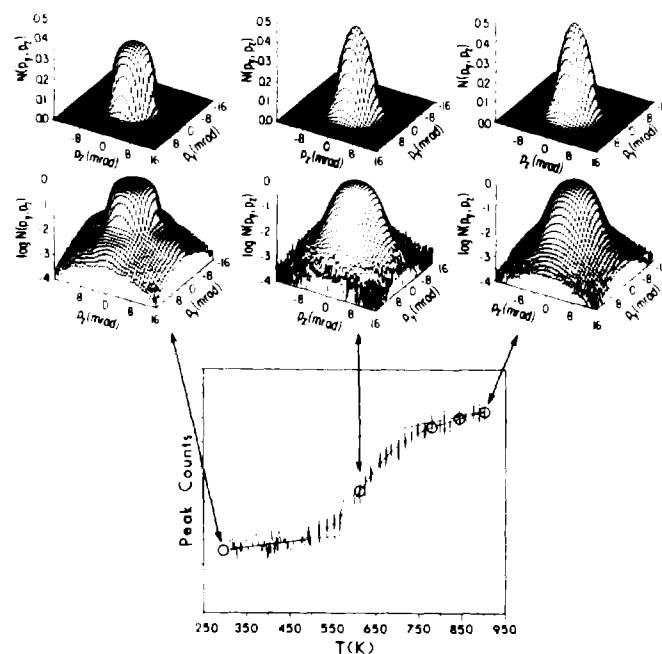
Fig. 1: Experimental 2D-ACAR surfaces and a 1D-ACAR peak-count rate result for Al single crystal [1,2].

parameter exhibits a greater slope at high temperature than is observed for the temperature dependence of the Bloch state seen at lower temperatures prior to the onset of the effect from thermally generated vacancy trapping sites.

Trapping model analyses of this data, assuming either monovacancies, or mono- and divacancies in the equilibrium population, reveal several important facts. First, that the temperature dependence of the trapped fraction is

independent of the model chosen. The reason for this is that such trapping model analyses fit to the trapping rate, which is independent of the partitioning of the positron among different traps, while the enthalpy and entropy parameters are quite sensitive to the model used. Second, it is observed that at the highest temperatures (>800 K), almost all the positrons are trapped, and hence even if one invoked a temperature dependent trapping rate or a temperature dependent vacancy formation entropy, it would have little influence on the peak-count rate temperature dependence. Finally, in consideration of relaxations around monovacancies, which might account for a strong temperature dependence; it is important to remember that the positron is very localized in the vacancy defect and cannot "see" beyond the nearest neighbors. The only existing model for such relaxations (6,7) proposes a 12.6 times greater expansion coefficient for monovacancies than for the lattice at 800 K; it is, however, a result of long-range atomic relaxations to which the trapped positron is likely insensitive. As a consequence of this temperature dependent behavior, variations are found in the deduced vacancy formation enthalpy particularly when comparisons are made between lifetime and momentum (Doppler broadening or ACAR) measurements (1,2,8).

2. THEORY

The calculated spectra are based upon a self-consistent pseudopotential scheme including electron-positron correlation applied to a superlattice of defects. The electronic structures for monovacancies and divacancies were calculated using the self-consistent pseudopodential method, in which the environments of the vacancy defects were simulated by a supercell containing 27 atom sites (9-11). No atomic relaxations around the vacancy defects were included although lattice expansion effects were. The self-consistency scheme was generalized to include positrons through a formalism based on a two-component density functional scheme (12). A norm-conserving ab initio pseudopotential was used for the electrons and a generalization of the pseudopotential scheme of Kubica and Stott (13) was used for the positron. The calculated spectra were folded with the experimental resolution and comparisons were made with the experimental data.

3. COMPARISONS

In Fig. 2 Radial <110> slices (points) through the experimental 2D-ACAR trapped-state spectra $N_+(903)$, $N_+(848)$, $N_+(773)$ and $N_+(613)$ are compared with <110> slices through the theoretical 2D-ACAR spectra for monovacancies (solid lines) and divacancies (dashed lines).
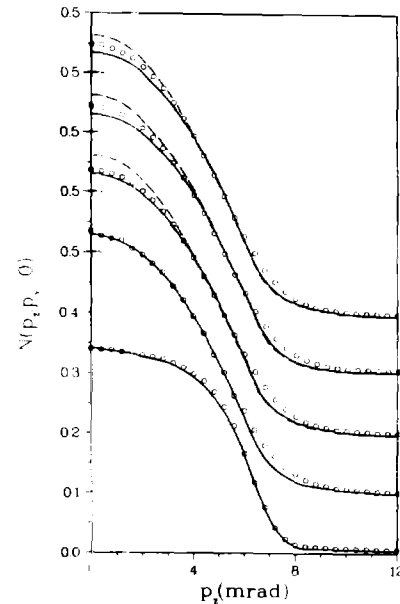

Fig. 2: Radial <110> slices through 2D-ACAR surfaces for theory and experiment.

The lowest curve is a comparison between the experimental results N(293) and the theoretical Bloch-state spectrum. These comparisons show that the theoretical calculations bracket the experimental results above 613K, implying an increasing fraction of the positrons annihilating from divacancies with increasing temperature. The trapped state spectra do, however, exhibit more smearing than the theory, likely a consequence of using a static model.

ACAR and Doppler broadening difference surfaces between Al at low temperatures (Bloch-state) and at high temperatures (defect-state) exhibit a double maximum. It is reasonable then to see if the theory used here reproduces this effect. Fig. 3a shows the difference between the $N_+(613)$ surface and N(293) while Fig. 3c is the difference between the theoretical monovacancy surface at 613 K and the theoretical Bloch state surface at 293 K ($N_{1v}(613)-N_B(293)$). Fig. 3e summarizes this comparison for a <110> slice with the points being the experiment and the line the theory. Similar comparisons are made for the 903 K surface in Figs. 3b,3d, and 3f. Here in Fig. 3f the comparison is made to both the monovacancy-Bloch, and divacancy-Bloch theoretical surface differences. As with the absolute comparison in Fig. 2, the experimental results are bracketed by the mono- and divacancy results. Earlier attempts to reproduce the double maximum had failed apparently because the theoretical spectra had all been calculated for the lattice constant at 0 K; the difference in the lattice constant between room temperature and the elevated temperatures where the effects from defects are present appears to be important in producing this effect.
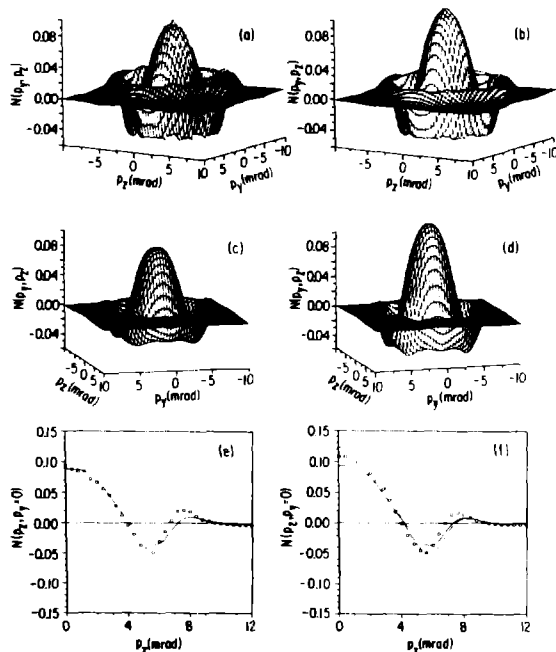
Fig. 3: Difference surfaces for theory and experiment.

Because the ACAR surfaces are linear combinations of the positron states it is possible to deduce the fraction of trapped positrons which annihilate from the divacancy state. The only uncertainty is that at 613 K we do not know exactly what fraction of the positrons might be in the divacancy-trapped state but the good agreement with theory suggests of the order of 0%. Table 1. (right-most column) summarizes the deduced values for the fraction of trapped positrons in the divacancy state I_{2v} as determined by the present ACAR results. I_{2v} may also be determined if one knows the concentration of mono- and divacancies and the ratio of the positron trapping rates into these sites. The concentrations have been obtained (14) from a fit to the concatenated data from previous differential dilatometry and post-quench resistometry measurements. This leaves only the trapping-rate ratio as a free variable. Table 1. demonstrates that by assuming this ratio to be of order 2 reasonable agreement is obtained with the present results, while if the ratio is 1 a significant discrepancy is seen. This conclusion is in reasonable accord with the results of the only theoretical calculations of this ratio (15,16).

$T(K)$	C_1	C_{1v}	C_{2v}	$I_{1v}\left(\frac{\mu_{2v}}{\mu_{1v}}=1\right)$	$I_{2v}\left(\frac{\mu_{2v}}{\mu_{1v}}=2\right)$	I_{2v}(2D ACAR)
613	7.99 × 10⁻⁶	7.54 × 10⁻⁶	2.27 × 10⁻⁷	0.03	0.06	0†
773	1.27 × 10⁻⁴	1.00 × 10⁻⁴	1.34 × 10⁻⁵	0.12	0.21	0.19
848	3.47 × 10⁻⁴	2.41 × 10⁻⁴	5.32 × 10⁻⁵	0.18	0.31	0.34
903	6.71 × 10⁻⁴	4.17 × 10⁻⁴	1.27 × 10⁻⁴	0.23	0.38	0.44

† This is an assumed value

Tbl. 1: The fraction of trapped positrons annihilating from divacancies deduced from ACAR and concatenated differential dilatometry and post quench resistivity.

REFERENCES

[1] M.J. Fluss, S. Berko. B. Chakraborty, K.R. Hoffmann, P. Lippel, and R.W. Siegel, J. Phys. F: Met. Phys. 14, 2831 (1984).

[2] M.J. Fluss, S. Berko. B. Chakraborty, P. Lippel, and R.W. Siegel, J. Phys. F: Met. Phys. 14, 2855 (1984).

[4] S. Berko in Positron Annihilation ed. R.R. Hasiguti and K. Fujiwara (Sendai: Japan Inst. of Met.) 65 (1979).

[5] S. Berko in Positron Solid-State Physics, Proc. Int. School of Physics 'Enrico Fermi' ed. W. Brandt and A. Dupasquier (N.Y.:North-Holland) 64 (1983).

[6] Ph Audit and H.M. Gilder, J. Nucl. Mater. 69-70, 641 (1978).

[7] Ph Audit in Point Defects and Defect Interactions in Metals ed. J. Takamura et al (Tokyo: Univ. of Tokyo Press) 278 (1982).

[8] G. Hood and R. Schultz, J. Phys. F: Met. Phys. 10, 575 (1980).

[9] B. Chakraborty, R.W. Siegel, and W.E. Pickett, Phys. Rev B 24, 5445 (1981).

[10] B. Chakraborty and R.W. Siegel in Point Defects and Defect Interactions in Metals ed. J. Takamura et al (Tokyo: Univ. of Tokyo Press) 93 (1982).

[11] B. Chakraborty, and R.W. Siegel, Phys. Rev. B 27, 4535 (1983).

[12] B. Chakraborty, Phys. Rev. B 24, 7423 (1981).

[13] P. Kubica and M. Stott, J. Phys. F: Met. Phys. 4, 1969 (1974).

[14] R.W. Siegel, J. Nucl. Mater. 69-70, 117 (1978).

[15] E. McMullen, R.J. Douglas, N. Etherington, B.T.A. McKee, A.T. Stewart, and A. Zaremba, J. Phys F: Met. Phys. 11, 1435 (1981).

[16] R.M. Nieminen, and J. Laakkonen, Appl. Phys. 20, 181 (1979).